Review of Scientific Instruments

The 3ω technique for measuring dynamic specific heat and thermal conductivity of a liquid or solid

Cite as: Review of Scientific Instruments **67**, 29 (1996); https://doi.org/10.1063/1.1146545
Submitted: 19 October 1994 • Accepted: 10 October 1995 • Published Online: 04 June 1998

I. K. Moon, Y. H. Jeong and S. I. Kwun

The 3ω technique for measuring dynamic specific heat and thermal conductivity of a liquid or solid

I. K. Moon and Y. H. Jeong[a)]
Department of Physics, Pohang University of Science and Technology, Pohang, Kyungbuk 790-784, South Korea

S. I. Kwun
Department of Physics, Seoul National University, Seoul 151-742, South Korea

(Received 19 October 1994; accepted for publication 10 October 1995)

We show how to measure dynamic specific heat and thermal conductivity of a solid or liquid sample using the 3ω technique, which is an ac-modulation method where we use a heater simultaneously as the sensor. By varying the width of the heater relative to the thermal decay length, one can choose the proper regime to measure thermal conductivity or specific heat. The technique is applied to window glass and the results confirm the validity of the method. Experimental results for potassium dihydrogen phosphate crystal demonstrate the first-order transition at the Curie point, and the dynamic specific heat of supercooled liquid potassium–calcium nitrate is shown. © *1996 American Institute of Physics.* [S0034-6748(96)03301-8]

I. INTRODUCTION

Measurements of thermal properties, specific heat, and thermal conductivity of condensed matter constitute one of the major characterizations of physical properties of condensed matter. Measurement of thermal conductivity of a solid, for example, offers a very nice way to investigate the elementary excitations, which participate as heat carriers or limit their mean free path in a given system. It also allows one to study mechanisms, such as defects in a crystal, which limit the mean free path of the heat carrying excitations. On the other hand, specific heat measurement allows one to directly monitor the free energy change of a given system as the external parameter such as temperature varies. This unique ability of specific heat measurements follows from the fact that specific heat per unit volume C_p is defined thermodynamically as

$$C_p=\frac{1}{V}\frac{dH}{dT}=\frac{T}{V}\frac{dS}{dT}, \tag{1}$$

where T, H, S, V are the temperature, the enthalpy, the entropy, and the volume of a given system, respectively.

In addition to the above, more traditional usage of the thermal measurements, one can use the specific heat measurements as a probe to the dynamics of a system, since specific heat is expressed as the enthalpy fluctuation of the system from the statistical mechanical point of view. Using the linear response theory,[1] it is fairly straightforward to define the dynamic, i.e., frequency-dependent specific heat $C_p(\omega)$ in terms of the time correlation function of the enthalpy of the system, namely,

$$C_p(\omega)=C_p^0+\frac{i\omega}{k_BT^2V}\int_0^\infty dt\ e^{i\omega t}\langle\delta H(0)\delta H(t)\rangle, \tag{2}$$

where k_B is the Boltzmann constant, C_p^0 is the usual static specific heat, and $\delta H(t)=H(t)-\langle H\rangle$ is the enthalpy fluctuation of the system. Although it is not common to actually observe the frequency-dependent specific heat, there are experimental situations where these dynamic specific heats were indeed measured. For example, Smith[2] observed the frequency-dependent specific heat in germanium and Smith and Holland[3] discussed it in terms of a delay in equilibrium. Frequency-dependent specific heat was also measured near the glass transition of glycerol[4] and potassium–calcium nitrate mixture.[5,6]

We have adopted the third harmonic detection method, an ac modulation method using the heater as a sensor simultaneously. The third harmonic detection method was originally discovered by Corbino long ago[7] and exploited extensively by Smith *et al.*[8] More recently Birge and Nagel[4] and Jung *et al.*[5] used a *planar* heater in applying the same method to probe the slow dynamics associated with the glass transition, while Cahill *et al.*[9] utilized a thin *line* heater to measure thermal conductivity of solids. In this article we shall call the calorimetric technique based on the third harmonic detection method a 3ω technique. We report our theoretical and experimental investigations of the 3ω technique applied to the general heat diffusion problem from a heater of arbitrary width. We show how the two regimes of planar and line types follow from the more general case and present experimental examples to display the validity and power of the technique.

II. THEORETICAL BASIS OF THE 3ω TECHNIQUE

In this section we lay down the theoretical basis of the 3ω method. We solve the problem for diffusion of heat into a medium from an oscillating heater located on the surface of the medium. We show that one can measure the specific heat and thermal conductivity of the medium, since the amplitude of the temperature oscillation of the heater itself contains the thermal information of the medium.

[a)]To whom all correspondence should be addressed.

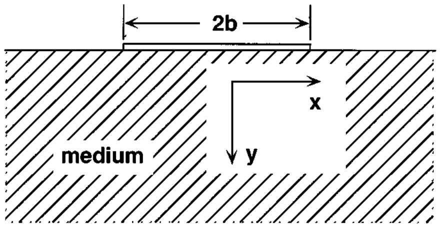

FIG. 1. Geometry of the heater and the medium. The medium is considered semi-infinite, and the heater of width $2b$ is regarded as a superposition of infinitely thin line heaters located between $x=-b$ and b. The heater is assumed to have a negligible mass and consequently no effect on the temperature profile of the medium.

A. Heat diffusion into a semi-infinite medium

Let us suppose that an infinitely long heater with a width $2b$ is placed on the surface of a semi-infinite medium as shown in Fig. 1, and it generates an oscillating power per unit length, $P_0 \exp(i2\omega t)$.[10] Using the result for an infinitely thin heater due to Carslaw and Jaeger[11] and remembering that the heater of width $2b$ can be regarded as a superposition of such thin heaters located between $-b$ and b,[9] we arrive at the expression for the complex amplitude of the temperature oscillation at the surface:

$$\delta T(x,y=0)=\frac{P_0}{\pi\kappa}\int_0^\infty \frac{\cos(kx)\sin(kb)}{kb(k^2+q^2)^{1/2}}\,dk, \tag{3}$$

where κ is the thermal conductivity and q is the complex thermal wave number defined as

$$q=\sqrt{\frac{i2\omega C_p}{\kappa}}. \tag{4}$$

It is noted here that the thermal oscillation decays exponentially in the y direction with a characteristic length, defined by various authors as the diffusion length, $\lambda=|q|^{-1}=\sqrt{\kappa/2\omega C_p}=\sqrt{D/2\pi}/\sqrt{2f}$, in which D is the thermal diffusivity. Because we shall use the heater as a sensor simultaneously (see Sec. III A), we calculate the temperature variation of the heater itself, δT_h, by taking the average of Eq. (3) from $-b$ to b, that is,

$$\delta T_h=\left(\frac{1}{2b}\right)\int_{-b}^{b}\delta T(x,y=0)\,dx$$

$$=\frac{P_0}{\pi\kappa}\int_0^\infty \frac{\sin^2(kb)}{(kb)^2(k^2+q^2)^{1/2}}\,dk. \tag{5}$$

Since the analytic expression of Eq. (5) is not known, one has to resort to the numerical calculation to find out the frequency dependence of δT_h. As an example we chose the medium to be window glass. Using the thermal diffusivity, $D=0.3$ mm^2/s, typical for window glass, we obtain $\sqrt{D/2\pi}=0.22$ mm s$^{-1/2}$, and $\lambda(\mu\text{m})=220\ \mu\text{m s}^{-1/2}/\sqrt{2f}$ where $f=\omega/2\pi$. Figure 2 is the calculated results for the heater of width $2b=440\ \mu$m. (This width was chosen somewhat arbitrarily for the sake of calculation.) Figure 2(a) shows that the magnitude $|\delta T_h|$ (in units of $P/\pi\kappa$) is linearly proportional to $\log 2f$ below 0.01 Hz, i.e., $\lambda>10b$. On the other hand, when $\lambda<b/10$, $\log|\delta T_h|$ is proportional to $\log 2f$ with the slope of $-1/2$ as is illustrated in Fig. 2(b). Figure 2(c) displays the phase as a function of frequency. It should be noted that the phase has a constant value of -45 deg at high frequencies.

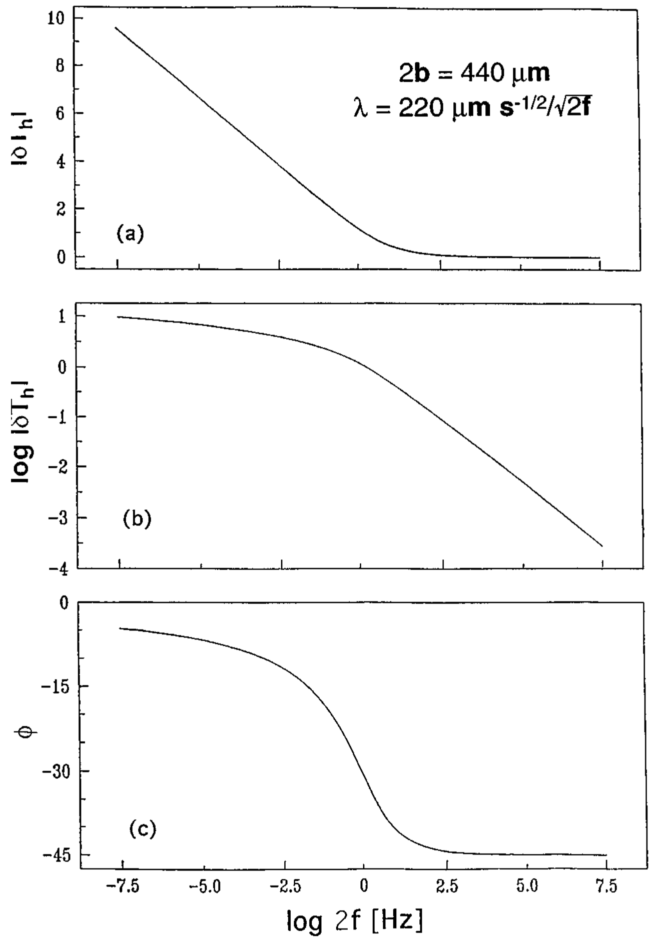

FIG. 2. The numerically calculated results for the heater of width $2b=440\ \mu$m. The thermal decay length was taken to be $\lambda(\mu\text{m})=220\ \mu\text{m s}^{-1/2}/\sqrt{2f}$, which is a typical value for window glass. Magnitude $|\delta T_h|$ of the heater oscillation is given in units of $P/\pi\kappa$, while the phase is in degrees.

It is easy to see how these numerical results follow from Eq. (5). If $b\ll\lambda$, the integral can be carried out by first setting $\sin(kb)/(kb)=1$. The result of integration is cast as

$$\delta T_h=\frac{P_0}{\pi\kappa}\left[-\ln\left(\frac{i2\omega b^2}{D}\right)^{1/2}+\eta\right]$$

$$=-\frac{P_0}{2\pi\kappa}\ln 2\omega-\frac{P_0}{2\pi\kappa}\ln\left(b^2\frac{C_p}{\kappa}\right)$$

$$-i\frac{P_0}{4\kappa}+\frac{\eta P_0}{\pi\kappa}, \tag{6}$$

where η is a constant having the value of 0.922... . Note that δT_h, more accurately its real part, $\mathrm{Re}[\delta T_h]$, is indeed linearly proportional to the logarithm of the measuring frequency. Since the coefficient of this linear term is inversely proportional to the thermal conductivity, one can obtain the thermal conductivity from the slope if one measures $\mathrm{Re}[\delta T_h]$ as a function of frequency in this regime. Thus it offers a way to measure thermal conductivity of a medium with a relatively small temperature gradient by taking advantage of the well-established power of the ac modulation technique.

For the opposite case of $b \gg \lambda$, one can use a mathematical identity for the Dirac delta function[12]

$$\lim_{b\to\infty} \frac{1}{\pi b} \left[\frac{\sin bx}{\sin x}\right]^2 = \delta(x) \tag{7}$$

to obtain from Eq. (5),

$$\delta T_h = \frac{P_0/2b}{\kappa q} = \frac{P_0/2b}{\sqrt{2\omega C_p \kappa}} e^{-i\pi/4}, \tag{8}$$

where $P_0/2b$ is now the power per unit area (or one can easily solve the one-dimensional heat diffusion problem to obtain the same result). By working in this regime, one can measure the product of specific heat and thermal conductivity, $C_p\kappa$, of the medium. Therefore, in principle by changing the measuring frequency to cover both regimes, one can obtain the thermal conductivity as well as the specific heat of the medium separately. In addition, if the specific heat becomes frequency dependent, the magnitude and phase of δT_h would follow Eq. (8) with the complex, instead of real, $C_p(2\omega)$ as defined in Eq. (2). Thus the dynamic specific heat can be obtained by measuring δT_h as a function of frequency.

B. Heat diffusion into both sides

When one deals with a liquid sample, one needs to evaporate a heater on a thick glass substrate. In this case the thickness of the substrate (like a solid sample) should be much greater than λ to avoid boundary effects from the back. A liquid sample is then put on top of the surface of the substrate. Now that there exist two different media on opposite sides of the heater, i.e., a glass substrate and a liquid sample, we have to extend the previous results. For the planar heater, it is straightforward, since the symmetry of the boundary matches that of the one-dimensional heat diffusion, to show that Eq. (8) becomes

$$\delta T_h = \frac{P_0/2b}{\sqrt{2\omega C_{pg}\kappa_g} + \sqrt{2\omega C_{pl}\kappa_l}} e^{-i\pi/4}, \tag{9}$$

where the subscripts g and l stand for glass and liquid, respectively.

In case of a line heater, on the other hand, it may not be possible to solve the heat diffusion equation exactly. However, if we neglect the boundary mismatch,[13] the problem can be written as a combination of two separate heat diffusions and, by defining $F(x) \equiv -\ln x + \eta$, δT_h is given as

$$\delta T_h = \frac{P_0}{\pi(\kappa_g + \kappa_l)} F(q_l b) \times \left[\frac{1}{1 + [\kappa_g/(\kappa_l + \kappa_g)](F(q_l b)/F(q_g b) - 1)}\right], \tag{10}$$

where q_l and q_g denote the complex wave numbers for the liquid and the glass, respectively. Since the quantity in the bracket is very slowly varying with temperature, one can still obtain the sum of thermal conductivities from the slope of δT_h versus $\log 2f$ (see Sec. IV). Thus, the glass contribution plays the role of background in both cases. To obtain the background information, one must carry out the measurements for the empty cell before taking data with samples.

III. EXPERIMENT

To implement above ideas into experimental reality, a method must be devised to detect the temperature variation of the heater itself. Also it becomes necessary to vary the width of the heater to cover the necessary range of b/λ, since the dynamic range needed to cover both regimes for a heater with a given width is far greater (14 decades) than is available experimentally. Finally, the experimental situation is expected to be different from the one where the heat diffusion equation was solved. For example, we assumed that the metallic heater on top of the sample would not affect the temperature profile in the sample. Also the length of the heater will be finite instead of infinite as assumed. The ultimate justification of these assumptions can only be made through experimental test. The first and second points are dealt with in this section, while the last point is discussed in Sec. IV.

A. Third harmonic detection

In order to measure the temperature oscillation of a heater itself we use the aforementioned third harmonic detection method, which is briefly described here.[8] If one drives the heater with a current at frequency ω, $I(t) = I_0 \cos \omega t$, then one gets Joule heating at frequency 2ω at the heater[14] and thus the temperature of the heater oscillates at the same frequency with the complex amplitude δT_h as given in the previous section. Since the heater is made of a metal such as gold or silver, its temperature coefficient of resistivity, $\alpha \equiv (1/R)(dR/dT)$, is not zero and as a result its resistance also oscillates at frequency 2ω. Thus,

$$R(t) = R_0[1 + \alpha|\delta T_h|\cos(2\omega t + \phi)], \tag{11}$$

where ϕ represents the phase shift of δT_h with respect to the power oscillation.

Due to the driving current $I(t)$ through the heater, the voltage across the heater appears as

$$\begin{aligned} V(t) &= I(t)R(t) = I_0 \cos \omega t \cdot R_0[1 + \alpha|\delta T_h|\cos(2\omega t + \phi)] \\ &= I_0 R_0 \cos \omega t + \tfrac{1}{2} I_0 R_0 \alpha |\delta T_h| \cos(\omega t + \phi) \\ &\quad + \tfrac{1}{2} I_0 R_0 \alpha |\delta T_h| \cos(3\omega t + \phi). \end{aligned} \tag{12}$$

It is the second and third terms that contain the thermal information of the sample we want to measure. Note, however, that they are relatively small compared to the first term since $\alpha \approx 0.004\ \mathrm{K}^{-1}$ and $|\delta T_h|$ is usually kept less than 20 mK to stay in the linear regime.

However, the last term, while small, appears at the third harmonic of the driving frequency and one can take advantage of this fact to measure the magnitude and the phase of the small signal in the presence of much larger unwanted signal using the Wheatstone bridge. The actual experimental

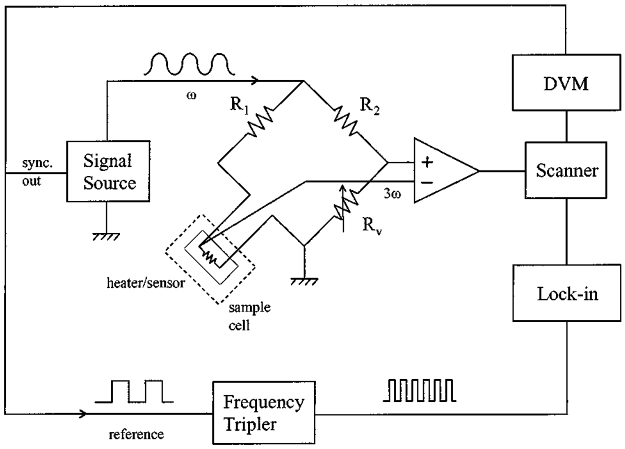

FIG. 3. Schematic diagram of the measuring circuit adopting the Wheatstone bridge. R_1 is a manganin wire with small temperature coefficient of resistivity, and the resistances of R_2 and R_v are a few orders of magnitude larger than those of the left-arm resistances of the bridge. The scanner toggles the signal between the digital voltmeter (DVM) and the lock-in amplifier for below and above 1 Hz measurements, respectively. Note that the three-probe method is used to remove the lead effects in balancing the bridge.

setup, which makes use of the Wheatstone bridge operated with a frequency synthesizer, is shown in Fig. 3. The technical details were described in Ref. 5.

B. Heater deposition on samples

Since the frequency range available with the third harmonic detection scheme is limited generally from 0.01 Hz to 5 kHz, one has to vary the width of the heater to bring the experimental frequency window into the proper regime. (The upper limit comes from the requirement that the common mode rejection ratio of the differential preamplifier be greater than 120 dB due to the small 3ω signal level, while the low-frequency limit is given by the maximum time one can wait at a given condition.) The heaters with varying widths were obtained by thermally evaporating either gold or silver onto the polished surfaces of samples or substrates (for a liquid) through the masks whose patterns are shown in Fig. 4. The typical thickness of a heater was ~1000 Å. This thickness was dictated by the conditions that the heater must be thin enough to be $\ll\lambda$ (otherwise one would be measuring the heater properties) and to disturb the temperature profile in the sample as little as possible. The length of line heaters were typically ~6 mm, while the width was varied down to 12 μm. In the case of plane heaters, we used the zigzag pattern as shown in Fig. 4(b) to obtain a reasonable value of resistance. Both the length of a heater and the thickness of a sample are required to be much greater than λ to satisfy the conditions assumed in solving the heat diffusion equation.

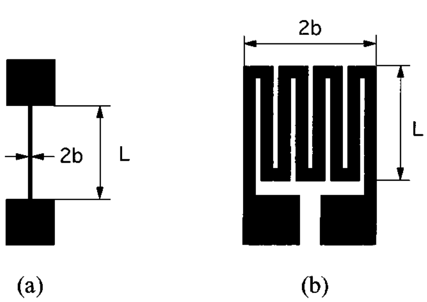

FIG. 4. The mask patterns used to produce line (a) and planar (b) heaters. The length (l) of the line heater is ~6 mm, while the width varies ($2b$). As for the plane heater, the line thickness, the total width ($2b$), and the length (l) are ~400 μm, 4 mm, and 6 mm, respectively.

IV. RESULTS AND DISCUSSION

In this section, we shall present experimental examples. These examples were chosen to show that the 3ω method is indeed an excellent way of measuring thermal properties of a medium. The first example serves to confirm the validity of the method, while the last two display the power of the method.

A. Test of the method: Thick window glass

To test the validity of the method, we made several samples of thick window glass (thickness$=$1 cm$\gg\lambda$) deposited with heaters of varying width and checked if Eq. (5) was obeyed as a function of frequency. Measurements were done in the neighborhood of room temperature. To obtain the magnitude of δT_h, which is necessary to calculate C_p and κ, from the measured voltage signal, the knowledge of α in Eq. (12) is required. In the 3ω method, the resistance of the heater is automatically obtained in the course of the experiment, since the bridge is balanced at each temperature, and this allows one to calculate α. Figures 5(a) and 5(b) show the magnitude of δT_h versus logarithm of measuring frequency on linear and logarithmic scales for the glass samples with heaters of various width. The lines in the figure were generated numerically from Eq. (5) using the known values of C_p and κ of glass. It is obvious from the figure that the agreement between the experimental data and the calculated values are fairly good for all cases. Especially encouraging is the obedience of the data to Eqs. (6) and (8) in the two extreme regimes ($2b=12$ μm and 4 mm) as can be seen in Figs. 5(a) and 5(b), since one would be largely working in these regimes where the interpretation of data is simple. When the width of the heater is in the middle, the crossover is seen as is predicted from Eq. (5).

To further confirm this obedience we have measured the absolute phase of the 3ω signal. This was done by calibrating the phase shifts of measuring circuits such as the preamplifier, lock-in amplifier, and the frequency tripler for the high-frequency measurements. Only the calibration of the preamplifier shift was necessary for the low-frequency data taken digitally with a digital voltmeter. The phase data and calculated values are compared in Fig. 5(c). Here again the agreement is excellent. Thus, these measurements provide the justification for the assumptions we made in Sec. II, the most critical of which was the unknown effect of the heater on the temperature profile in the sample. Now one can be fairly confident about the capability of the 3ω method as a tool for the measurement of thermal properties of a solid. Also we have shown that, even if the two extreme regimes give rise to simple interpretation of data, it is still possible to deal with the finite-size effects utilizing the general expression, Eq. (5).

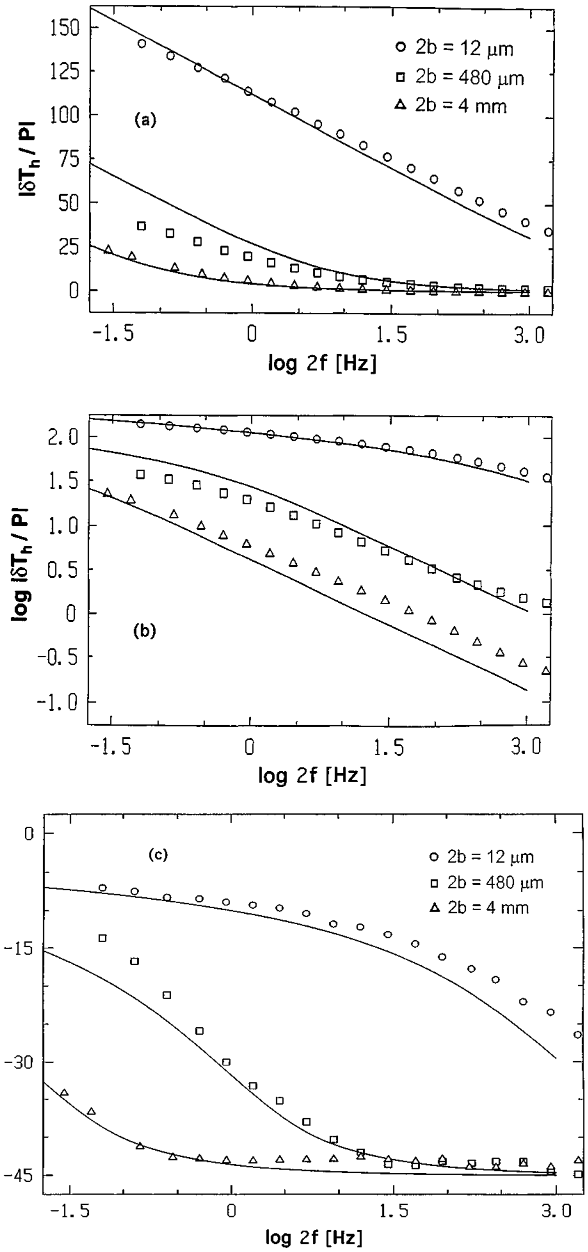

FIG. 5. Amplitude of temperature oscillation, δT_h, of the heaters of various widths on thick window glass vs the logarithm of measuring frequency $2f$: (a) $|\delta T_h/P|$ vs $\log 2f$, (b) logarithm of $|\delta T_h/P|$ vs $\log 2f$, (c) the absolute phase of δT_h vs $\log 2f$. The widths $(=2b)$ of the heaters are indicated in the figure. In (a) and (b), $|\delta T_h/P|$ (in units mK and mW, respectively) is plotted since the power level was changed as the measuring frequency varied.

B. Results for a solid: KDP

KH_2PO_4 (KDP) crystals were grown from an aqueous solution kept at 35 °C. The samples used in the measurements had typical dimensions of 10×10×10 mm. The thickness was much larger than the thermal decay length, λ, in the frequency range used in the experiment and this fact ensured that the boundary did not perturb the thermal diffusion. Figure 6 is the plot of the thermal conductivity κ of KDP as a function of temperature measured by the 3ω method with a line heater deposited on the (010) surface. The width of the line heater was 80 μm and measuring frequencies were below 12 Hz. κ was obtained from the slope in the graph of Re[δT_h] versus logarithm of measuring frequency at each temperature. In the ferroelectric phase, κ decreases sharply with increasing temperature, while in the paraelectric phase κ increases slowly as the temperature is raised. The inset displays a small but abrupt jump in κ at the Curie point (T_c) 居里点 indicating the first-order nature of the transition. The detailed behavior of the thermal conductivity of KDP and the related physics are discussed in Ref. 15. Measurements with a planar heater were also performed and the data from the planar configuration were used to calculate $C_p\kappa$ according to Eq. (8). $C_p\kappa$ so obtained was divided by κ to yield the specific heat, C_p. Figure 7 is the plot of $C_p\kappa$ and C_p of KDP measured at 0.2 Hz of temperature oscillation. C_p shows a familiar peak associated with the ferroelectric phase transition and this result agrees fairly well with the previous measurements.[16]

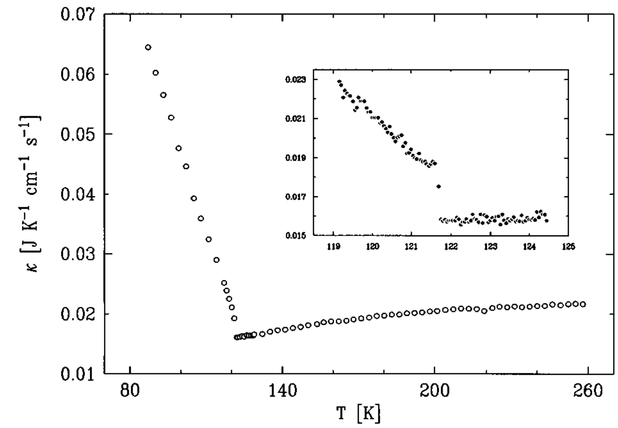

FIG. 6. The thermal conductivity of KDP as a function of temperature measured by the 3ω method. κ of KDP displays a discontinuity at the Curie point T_c as the inset illustrates.

C. Results for a liquid: CKN

$(Ca(NO_3)_2)_{0.4}(KNO_3)_{0.6}$ (CKN) is an ionic liquid which can be easily supercooled. When a liquid is supercooled without crystallization, a slow relaxation phenomenon occurs and the dynamic specific heat can be observed.[4,6] We used

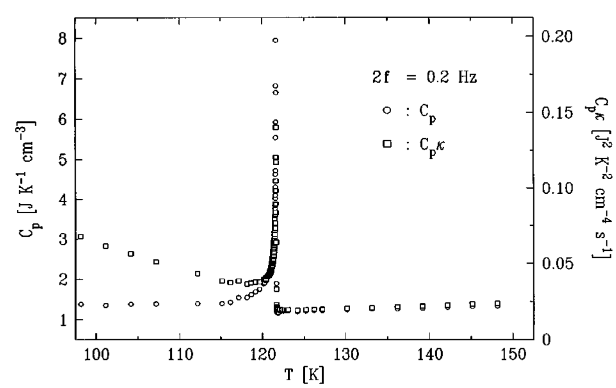

FIG. 7. $C_p\kappa$ (square) and C_p (circle) of KDP as a function of temperature measured at 0.2 Hz (twice heating-current frequency) by the 3ω method with a planar heater. The decrease of $C_p\kappa$ in the ferroelectric phase, as T increases, is due to the decrease of κ.

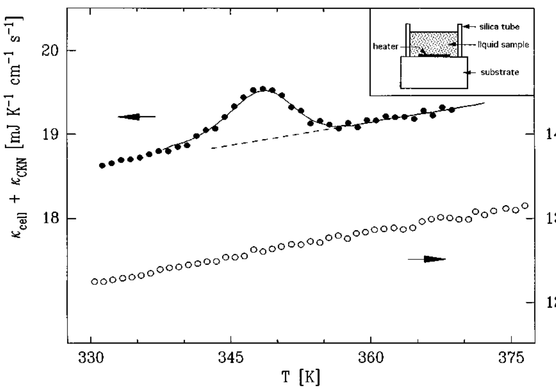

FIG. 8. Thermal conductivity of the cell, κ_{cell}, and the total conductivity, $\kappa_{cell}+\kappa_{CKN}$, obtained from the slope of Re[δT_h] of the line heater against $\log 2f$ are plotted as a function of temperature. The peak in $\kappa_{cell}+\kappa_{CKN}$ is solely due to the frequency dependence of C_p of CKN, while the linear part is due to the cell contribution. The solid line represents the calculated values according to Eq. (10) assuming that the thermal conductivity of CKN, κ_{CKN}, is constant. Thus, κ_{CKN} is essentially constant and the true total conductivity is indicated by the broken line. Inset shows the liquid sample cell.

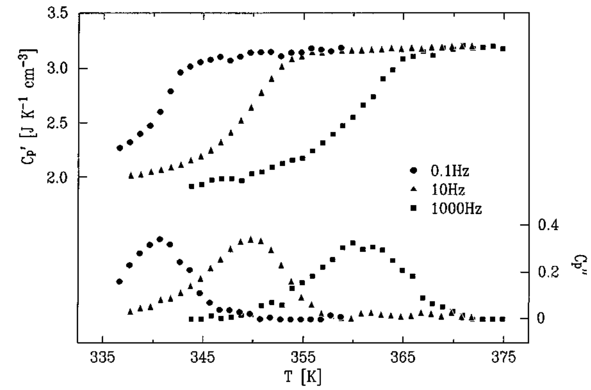

FIG. 9. Real and imaginary parts of the dynamic specific heat of CKN at various frequencies are displayed as a function of temperature. The frequencies indicated in the figure are those of the temperature oscillation, i.e., twice the heating frequencies. The frequency-dependent behaviors of C_p of CKN are those seen in typical relaxations.

the 3ω method to measure the thermal conductivity and the dynamic specific heat in the supercooled state of CKN. Since the sample is liquid, we evaporated a heater on a glass substrate and put a short silica glass tube with the diameter slightly larger than the size of the heater as shown in the inset of Fig. 8. A small amount of CKN was put into the tube and melted.

Figure 8 displays the thermal conductivity data of the empty sample cell and CKN as a function of temperature. They were obtained from the slope of Re[δT_h] against $\log 2f$ for the empty and liquid-filled cell with a line heater of width 60 μm according to Eqs. (6) and (10). While κ_{cell} shows a linear behavior in temperature, κ_{CKN} displays a peculiar peak around 350 K. This behavior can be understood if we take into consideration the frequency dependence of C_p of CKN. When C_p is a frequency-independent, real quantity at high and low temperatures, the term in the bracket of Eq. (10) shows little frequency dependence and its effect on the coefficient of $\log 2f$ is negligible ($\sim$0.05%). Thus, the slope gives rise to correct, total thermal conductivity of the cell and the sample. However, when C_p of CKN becomes frequency dependent, the coefficient of $\log 2f$ obtained from the blind linear fitting of the δT_h data yields an erroneous value for the thermal conductivity and one has to use the full expression of Eq. (10). In other words, the frequency dependence of C_p, which in turn makes the term in the bracket of Eq. (10) frequency dependent, does not allow the simple intepretation. If one insists the linear relationship between Re[δT_h] and $\log 2f$, then the coefficient is no longer inversely proportional to thermal conductivity.

To account quantitatively for the peak around 350 K, we calculated Re[δT_h], as a function of frequency, according to Eq. (10) by assuming κ of CKN is constant and using the $C_p(2\omega)$ values of CKN in Fig. 9. Then we obtained the coefficient of $\log 2f$ by linear fitting the calculated Re[δT_h] values against $\log 2f$. The solid line of Fig. 8 represents the results and it is in full agreement with the data. This fact clearly demonstrates that κ of CKN is essentially temperature independent.

Figure 9 shows the dynamic specific heat, $C_p(2\omega)$, of CKN as a function of temperature at various frequencies. These values of $C_p(2\omega)$ were obtained by dividing the planar heater data, $C_p(2\omega)\kappa$, with the constant value of κ of CKN from Fig. 8. $C_p(2\omega)$ shows a typical relaxation behavior of a supercooled liquid as is often seen in dielectric measurements. In other words, the real part shows dispersion and the imaginary part a peak as a result of the characteristic time of the system matching the probing time (=inverse frequency). The physics related to this behavior is discussed elsewhere.[6]

ACKNOWLEDGMENTS

This work was conducted with 1993 nondirected research fund of Korea Research Foundation, and the financial supports from Basic Science Research Institute of Pohang University of Science and Technology and Research Center for Dielectric and Advanced Matter Physics of Pusan University.

[1] R. Kubo, Rep. Prog. Phys. **29**, 255 (1966).
[2] R. C. Smith, J. Appl. Phys. **37**, 4860 (1966).
[3] R. C. Smith and L. R. Holland, J. Appl. Phys. **37**, 4866 (1966).
[4] N. O. Birge and S. R. Nagel, Rev. Sci. Instrum. **58**, 1464 (1987).
[5] D. H. Jung, T. W. Kwon, D. J. Bae, I. K. Moon, and Y. H. Jeong, Meas. Sci. Technol. **3**, 475 (1992).
[6] Y. H. Jeong and I. K. Moon, Phys. Rev. B **52**, 6381 (1995).
[7] O. M. Corbino, Phys. Z. **12**, 292 (1911).
[8] L. R. Holland, J. Appl. Phys. **34**, 2350 (1963); D. Gerlich, B. Abeles, and R. E. Miller, *ibid.* **36**, 76 (1965); L. R. Holland and R. C. Smith, *ibid.* **37**, 4528 (1966).
[9] D. G. Cahill, H. E. Fisher, T. Klitsner, E. T. Swartz, and R. O. Pohl, J. Vac. Sci. Technol. A **7**, 1259 (1989); D. G. Cahill, Rev. Sci. Instrum. **61**, 802 (1990).
[10] The angular frequency 2ω is due to the fact that a current at ω through the heater produces Joule heating at 2ω. We take $\exp(i2\omega t)$, unlike Ref. 5, as a time-varying factor following Ref. 11.
[11] H. S. Carslaw and J. C. Jaeger, *Conduction of Heat in Solids* (Clarendon, Oxford, 1959), p. 193.
[12] G. Arfken, *Mathematical Methods for Physicists* (Academic, Orlando, 1985), p. 488.

[13] This is, of course, a crude approximation neglecting the heat transfer between the two media. In an experimental situation dealing with a liquid, however, this approximation is not as bad as it may appear. For example, the thermal decay lengths of substrate glass and potassium–calcium nitrate liquid in the last example of Sec. IV differ by only 20%.
[14] There also exists, due to the dc component of power, a constant shift of the sample temperature with respect to the bath temperature, but it can be easily calibrated away.
[15] D. J. Bae, K. B. Lee, Y. H. Jeong, S. M. Lee, and S. I. Kwun, J. Kor. Phys. Soc. **26**, 137 (1993); S. M. Lee, S. I. Lim, S. I. Kwun, and Y. H. Jeong, Solid State Commun. **88**, 361 (1993).
[16] W. Reese, Phys. Rev. **182**, 646 (1969).